Electronic Supplementary Material (ESI) for Environmental Science: Nano.

Supporting Information

Antifouling Properties of Two Dimensional Molybdenum Disulfide and Graphene Oxide

Iftaykhairul Alam [1], Linda M. Guiney[2], Mark C. Hersam[2], and Indranil Chowdhury [1*]

[1] Department of Civil & Environmental Engineering, Washington State University, Pullman, WA 99164, USA

[2] Departments of Materials Science and Engineering, Chemistry, and Medicine, Northwestern University, Evanston, Illinois 60208, USA

Number of Figures. 11

Number of Table. 1

*Contacting author: indranil.chowdhury@wsu.edu; 509-335-3721

1. Introduction

In this section, additional details on graphene oxide (GO) synthesis and DLVO theory are provided. Raw data from QCM-D are presented in the supporting information. Moreover, interaction energy profile between *E. coli* and GO/MoS_2 calculated from DLVO theory and mechanistic figure of NOM and *E. coli* interactions with the GO are also provided in the supporting information.

2. Synthesis of GO

As discussed, modified Hummer's was used to prepare GO. [1, 2] 115 ml concentrated sulfuric acid was placed in 2L beaker and cooled to 0°C using an ice water bath. 5 g of natural graphite flakes (3061 grade material from Asbury Graphite Mills) were added to acid followed by slow addition of 15g $KMnO_4$ with continuous stirring and cooling so that temperature does not go above 20°C. Heating the mixture to 35°C, 230 mL of deionized (DI) water was added and the reaction was ended after the addition of 700 mL of DI water. Finally, 12.5 mL of 30% H_2O_2 solution was slowly added to the mixture. The mixture was treated subsequently by vacuum filtration and 1:10 HCL solution to remove as much as liquid and metal contaminants respectively. After resuspension of the filtrate in 500 mL DI water, it was centrifuged for 12 h at 7500 rpm to sediment the GO, and the supernatant was decanted. After repeating the DI wash 6 times, the final solution resulted in mixture with pH of around 6. The mixture was further sonicated in stainless steel beakers via a Fisher Scientific Model 500 Sonic Dismembrator with a 1/2" tip for 1 hour at 50% amplitude (~55 W) while cooled in an ice water bath. Finally, any unoxidized graphite was removed by

centrifugation at 5000 rpm for 10 min. By slow evaporation of the liquid from a portion of the final solution, the optical absorbance at 300 nm was determined to be 3680 mL mg $^{-1}$ m $^{-1}$.

3. Derjaguin−Landau−Verwey−Overbeek (DLVO) theory

Previous studies have shown that the deposition and aggregation kinetics of NOM and other foulants present in 1-1 electrolyte solution (i.e. NaCl) on nanomaterials can be explained by colloidal theory including DLVO theory.[3,4] The DLVO theory explains the aggregation of aqueous dispersions quantitatively and describes the force between charged surfaces interacting through a liquid medium. It combines the effects of the van der Waals attraction and the electrostatic repulsion[4] The attraction (van der Waals) energy between a sphere and a flat plate at a separation distance of h, is defined as[4]:

$$V\text{VDW } in\, J = -\frac{Aa}{6h}\left[\frac{1}{1+\frac{14h}{\lambda}}\right] \qquad (4)$$

Where,

A = Hamaker Constant (J) where A= 5.80*10^{-21} J

a = colloid particle radius (m)

λ = dielectric wavelength (m)

The interaction energy between a sphere, with diameter 2a and an infinite plate, and zeta potentials of Ψ_1 and Ψ_2 respectively, separated by a distance h, by the Deryagin method is as follows[5]:

$$V_{EDL} in\, J = \pi a \varepsilon_o \varepsilon_r \left\{ 2\Psi_1 \Psi_2 ln\left(\frac{1+e^{-\kappa h}}{1-e^{-\kappa h}}\right) + \left(\Psi_1{}^2 + \Psi_2{}^2\right) ln\left(1-e^{-2\kappa h}\right) \right\} \qquad (5)$$

Where,

κ = debye length (m^{-1})

ε_o = permitivity of free space (C/Vm)

ε_r = relative permittivity

Ψ_1 = collector (plate) surface potential (V)

Ψ_2 = colloid (sphere) surface potential (V)

In this study, GO and MoS_2 coated gold sensors acted as plates while the *E. coli* cells were considered to be spheres. DLVO theory will help to understand the interaction of foulants with the material surfaces.

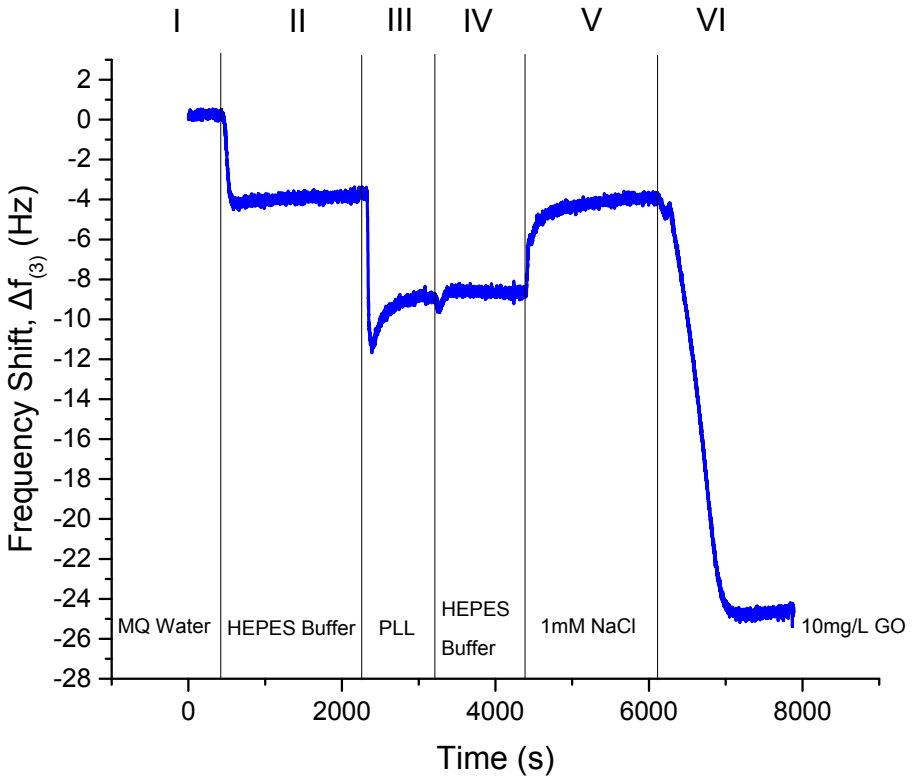

Figure S1. The gold sensor was rinsed with MQ water for at least 60 min (data not shown in the figure) to achieve a stable baseline before starting any fouling experiment (Stage I). Frequency shifts at the third overtone during deposition of negatively charged GO on a negatively charged gold surface using QCM-D with the help of a positively charged PLL polymer layer working as a linker between the gold surface and GO. A decrease in the frequency shift (stage II, III, VI) suggests the deposition of mass onto the gold surface and an increase (stage III, V) indicates release of mass.

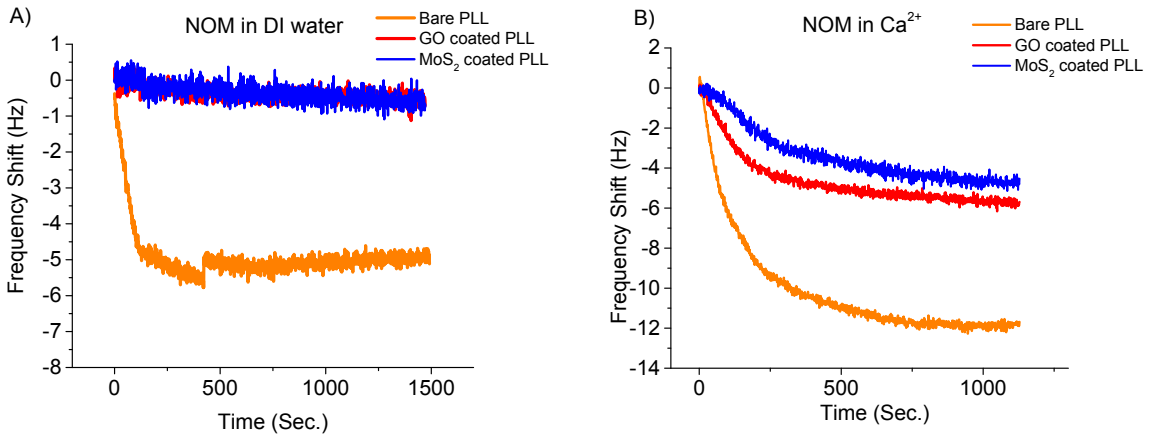

Figure S2. Interaction of PLL, GO and MoS_2 surfaces with NOM without any salts (Fig. A, left) and NOM in Ca^{2+} (Fig. B, right). PLL surface being positively charged showed higher fouling against negatively charged foulants. Moreover, lower frequency shifts and attachment efficiencies for GO and MoS_2 indicated there was no PLL exposed after GO/MoS_2 deposition. Any exposed PLL even after GO/MoS_2 coating would result into higher frequency shifts and dissipation changes like bare PLL surface experiment.

Table S1. QCM-D results

Fouling condition	Material surface	Maximum frequency shifts (Replicates)	Attachment efficiency (Replicates)
NOM without any salt	GO	-0.96 Hz -1.33 Hz -0.97 Hz	0.35 0.21 0.37
	MoS_2	-0.39 Hz -0.71 Hz -0.4 Hz	0.18 0.22 0.17
NOM in Na^+	GO	-1.88 Hz -1.84 Hz -1.48 Hz -1.38 Hz	0.61 0.65 0.41 0.60
	MoS_2	-1.79 Hz -1.38 Hz -1.35 Hz	0.34 0.35 0.39
NOM in Ca^{2+}	GO	-6.23 Hz -5.92 Hz -5.33 Hz	0.85 0.75 0.38
	MoS_2	-5.41 Hz -4.06 Hz -4.646 Hz	0.35 0.4 0.43
NOM in Mg^{2+}	GO	-5.73 Hz -4.21 Hz -5.38 Hz	0.84 0.69 0.75
	MoS_2	-2.93 Hz -4.66 Hz -3.89 Hz	0.47 0.41 0.33
E. coli in Na^+	GO	-6.95 Hz -6.08 Hz -9.13 Hz	0.72 0.61 0.81
	MoS_2	-4.22 Hz -6.58 Hz -4.22 Hz	0.69 0.67 0.42

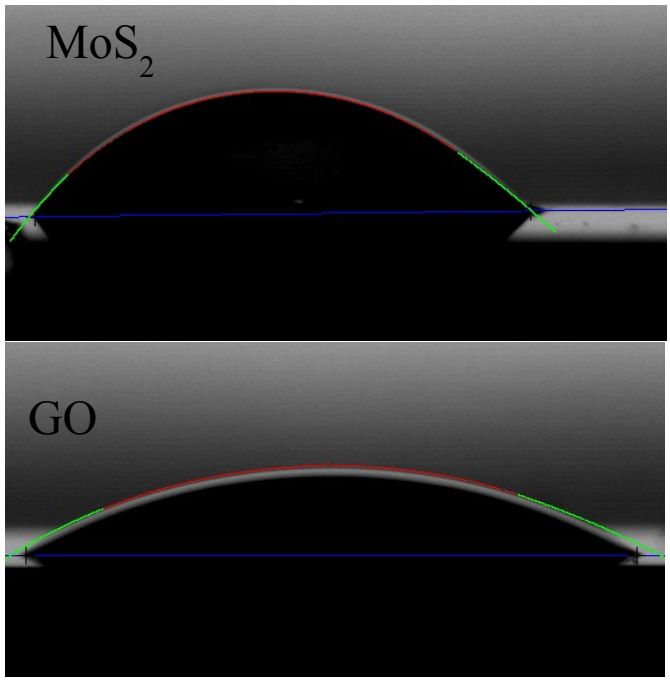

Sample	Contact Angle (°)
MoS_2	42 ± 4.6
GO	25 ± 5.4

Figure S3. Contact angle measurements of GO and MoS_2 on SiO_2 substrate.

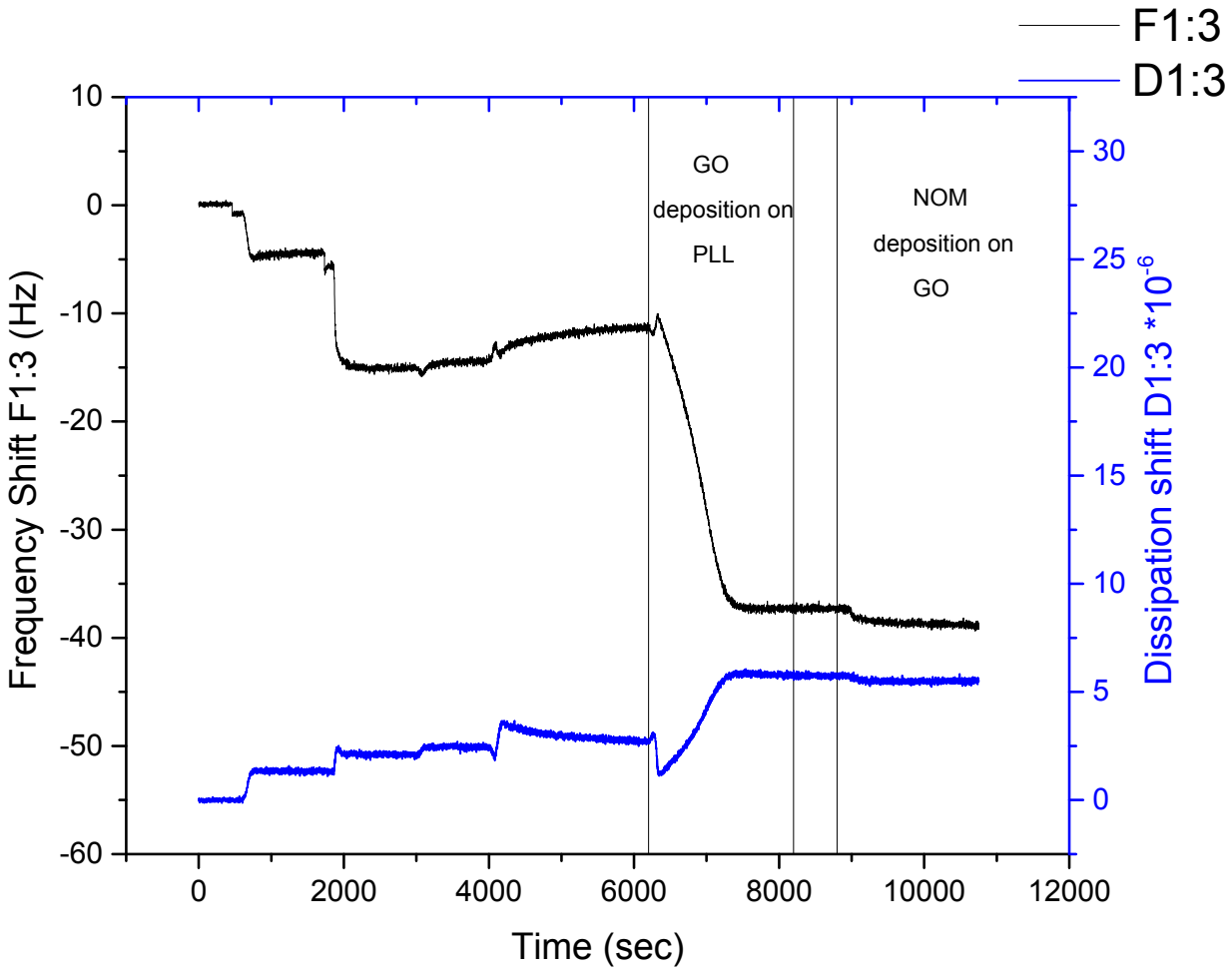

Figure S4. Real time data of the NOM deposition on a GO surface during different experiments acquired from QCM-D software tools Q-Tools. Small changes in frequency shift and dissipation energy indicates NOM deposition on GO surface. Here, F1:3 and D1:3 denote frequency shift and dissipation shift, respectively, on 3rd overtone during the NOM interactions with the material surface.

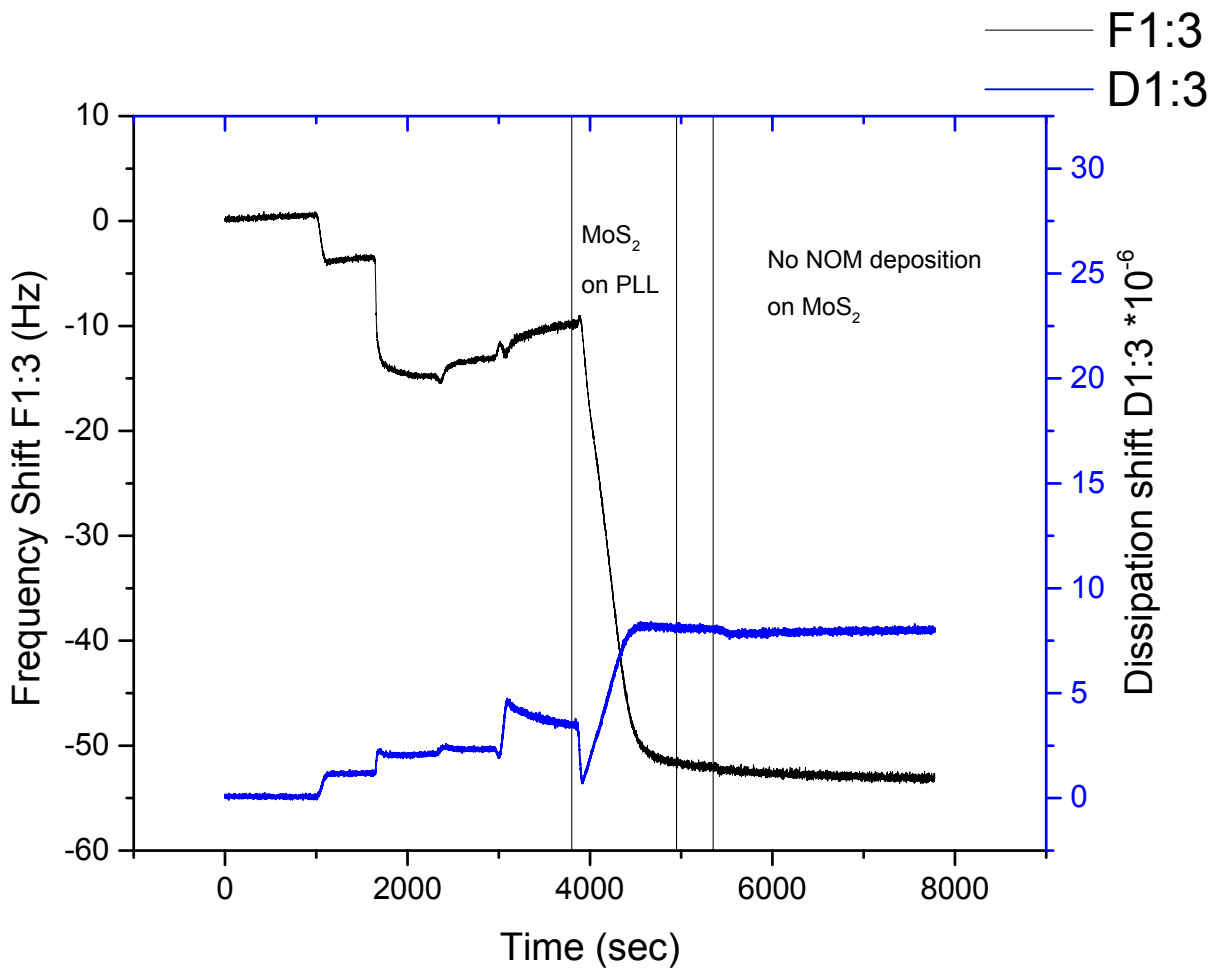

Figure S5. Real time data of the NOM deposition on a MoS_2 surface during different experiments acquired from QCM-D software tools Q-Tools. NOM showed hardly any change in frequency shift and dissipation energy during NOM deposition indicating no interaction of NOM with MoS_2 surface.

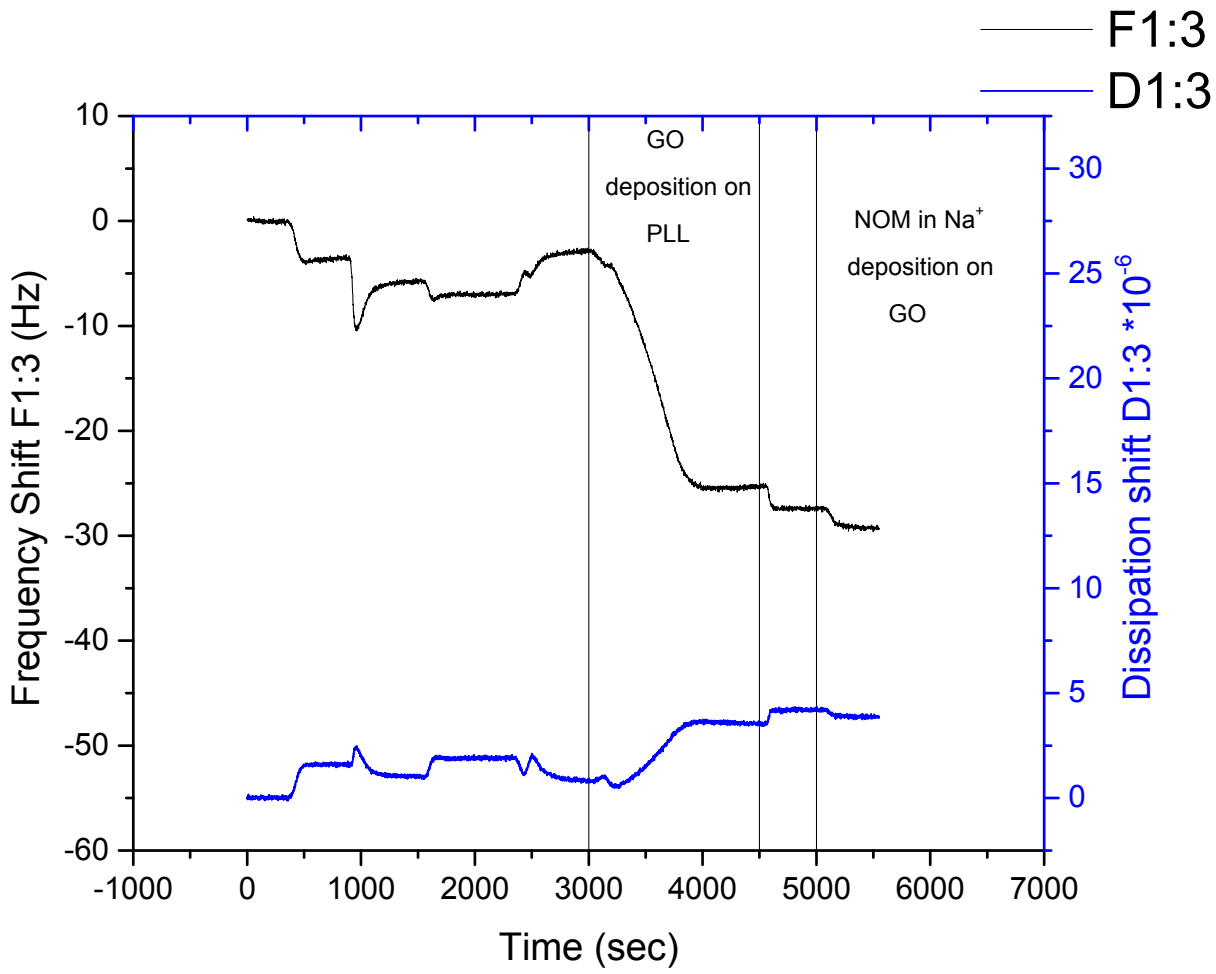

Figure S6. Real time data of the NOM in NaCl deposition on a GO surface during different experiments acquired from QCM-D software tools Q-Tools. NOM showed a slight change in frequency shift and dissipation energy during NOM deposition indicating interaction of NOM with the GO surface.

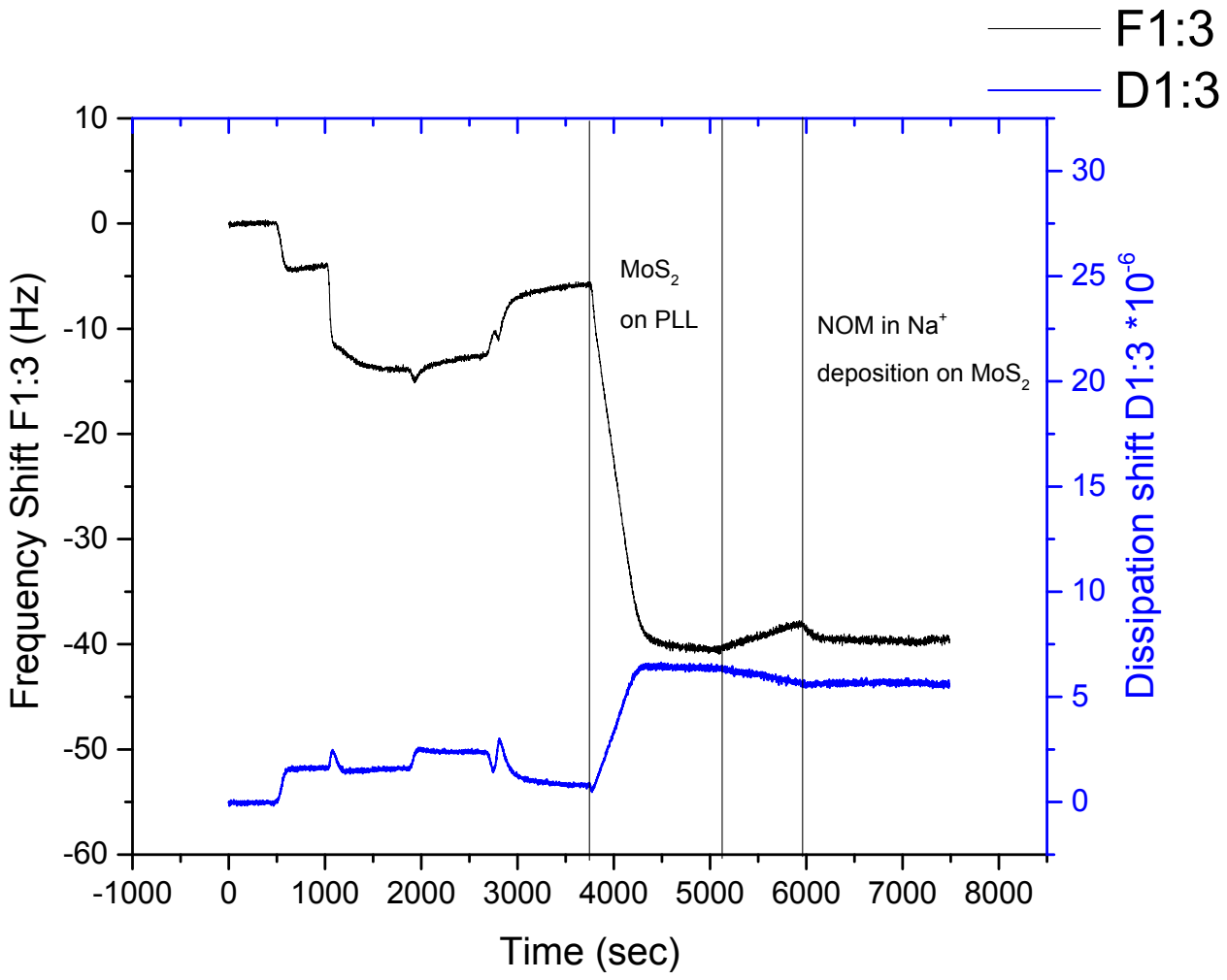

Figure S7. Real time data of the NOM in NaCl deposition on a MoS_2 surface during different experiments acquired from QCM-D software tools Q-Tools. NOM showed a slight change in frequency shift and dissipation energy during NOM deposition in the presence of the monovalent ion. Presence of NaCl in NOM increased the interaction of NOM with MoS_2.

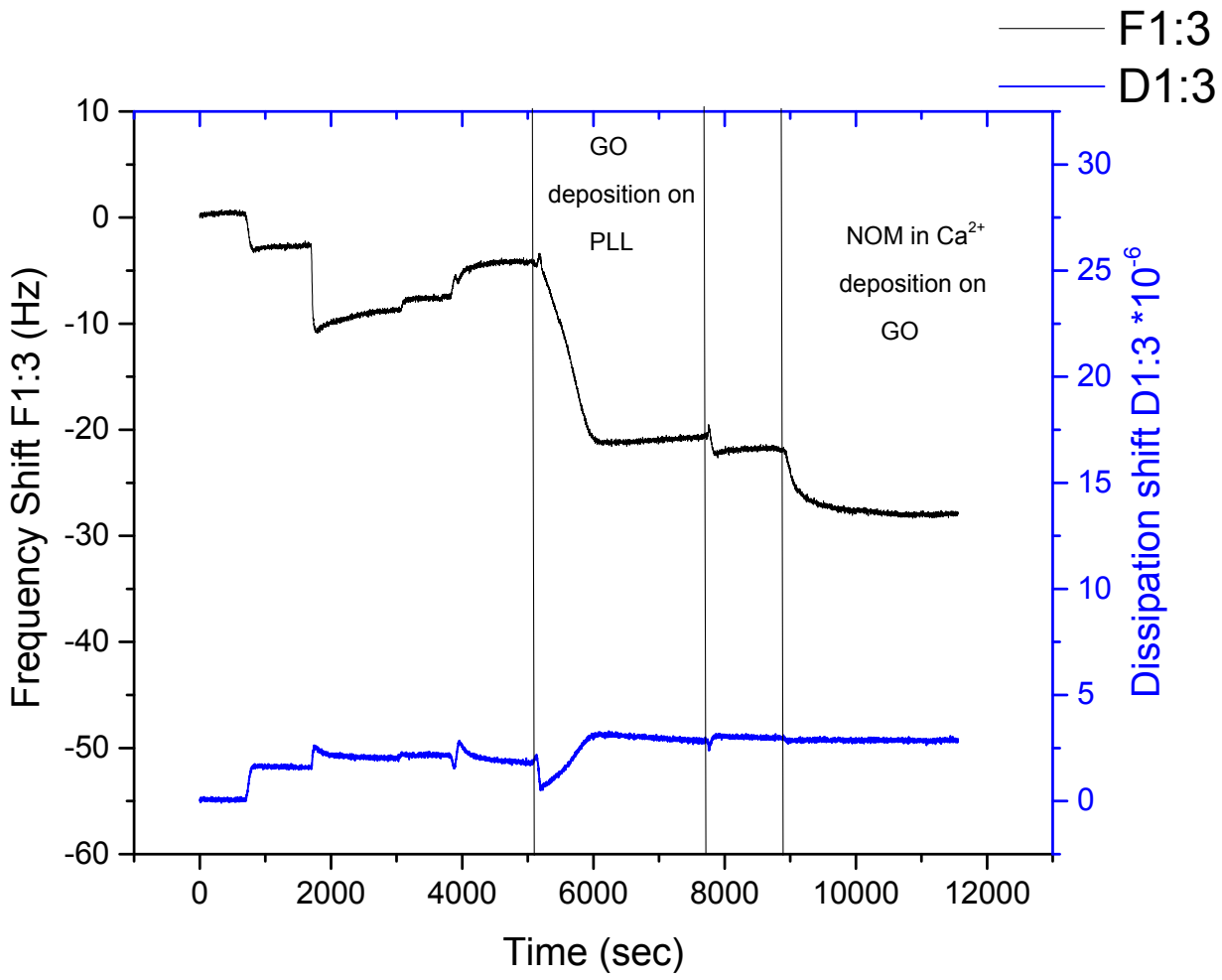

Figure S8. Real time data of the NOM in $CaCl_2$ deposition on a GO surface during different experiments acquired from QCM-D software tools Q-Tools. NOM showed a huge change in frequency shift and dissipation energy compared to NOM in NaCl during NOM deposition in the presence of the divalent cation. NOM in $MgCl_2$ showed a similar type of interaction with the GO surface.

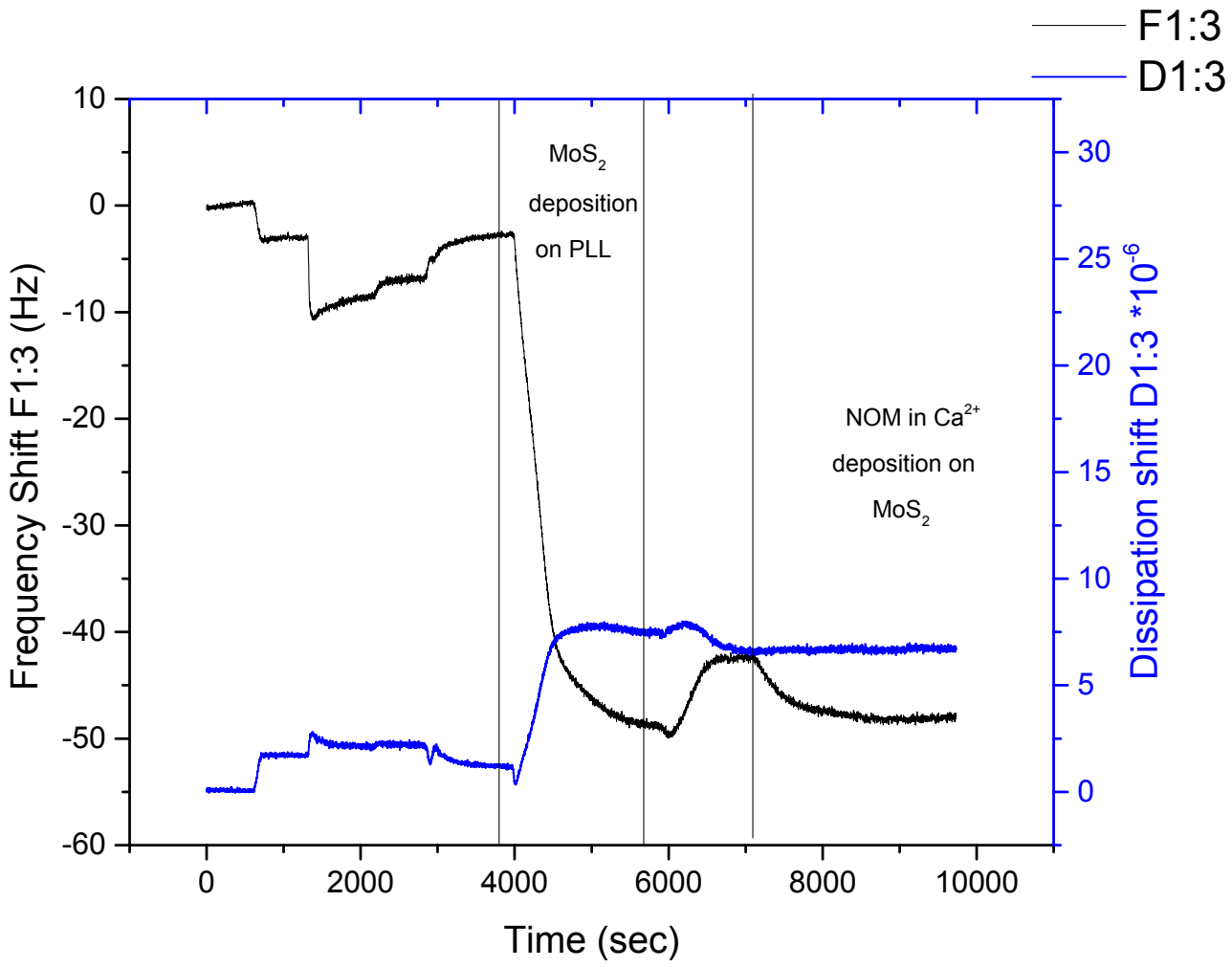

Figure S9. Real time data of the NOM in $CaCl_2$ deposition on a MoS_2 surface during different experiments acquired from QCM-D software tools Q-Tools. NOM in $MgCl_2$ showed a similar type of interaction with the MoS_2 surface. Similar to the GO surface, NOM in the presence of divalent cations showed higher deposition on the MoS_2 surface.

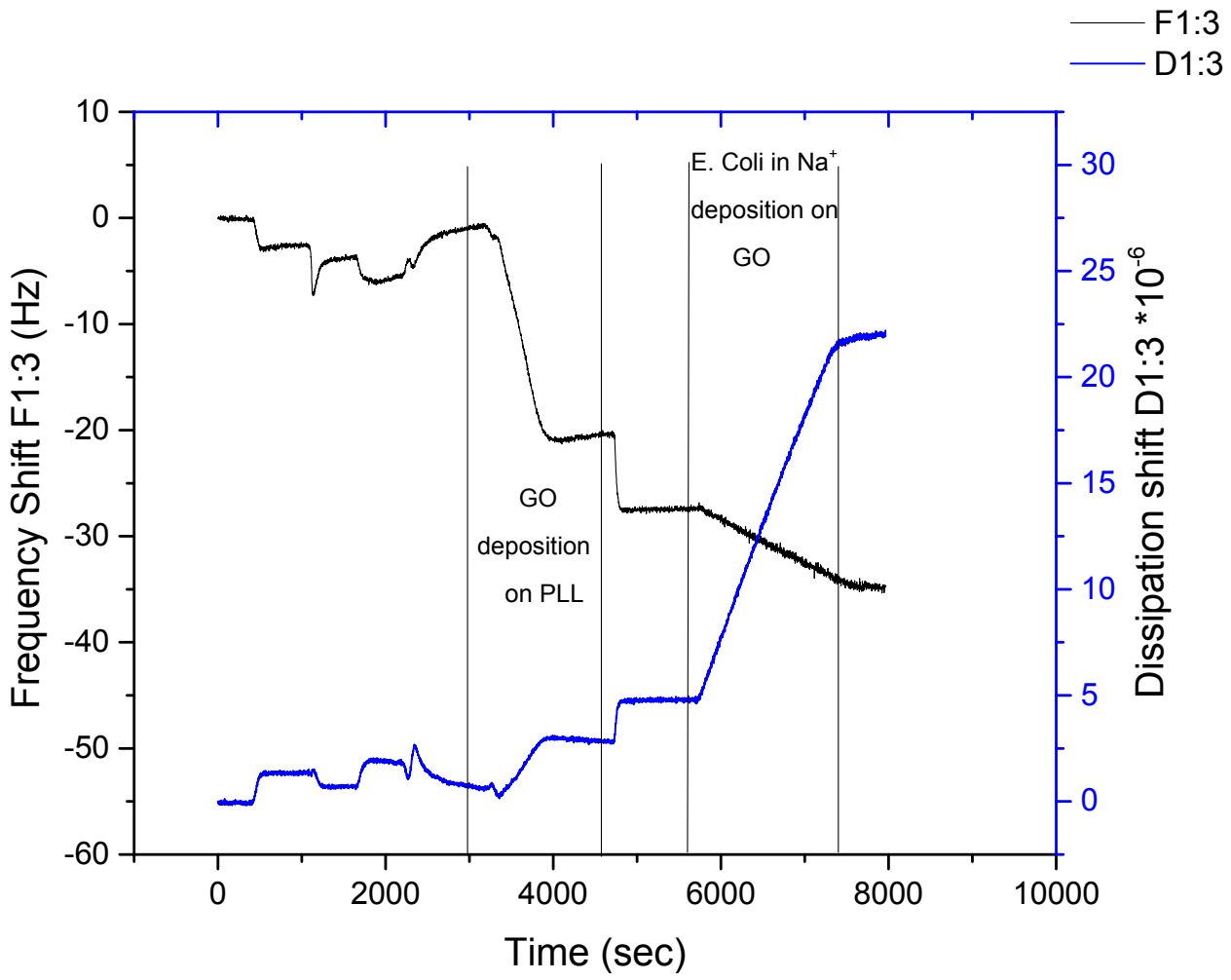

Figure S10. Real time data of the *E. Coli* in NaCl deposition on a GO surface during different experiments acquired from QCM-D software tools Q-Tools. *E. coli* deposited slowly but continuously for 30 min (change in frequency shift and dissipation energy) until the *E. Coli* injection was stopped and background salt solution was flowed (indicated by stabilization of frequency shift and dissipation energy). Unlike NOM, *E. Coli* showed a huge change in dissipation energy which indicates a softer layer is created by *E. Coli*.

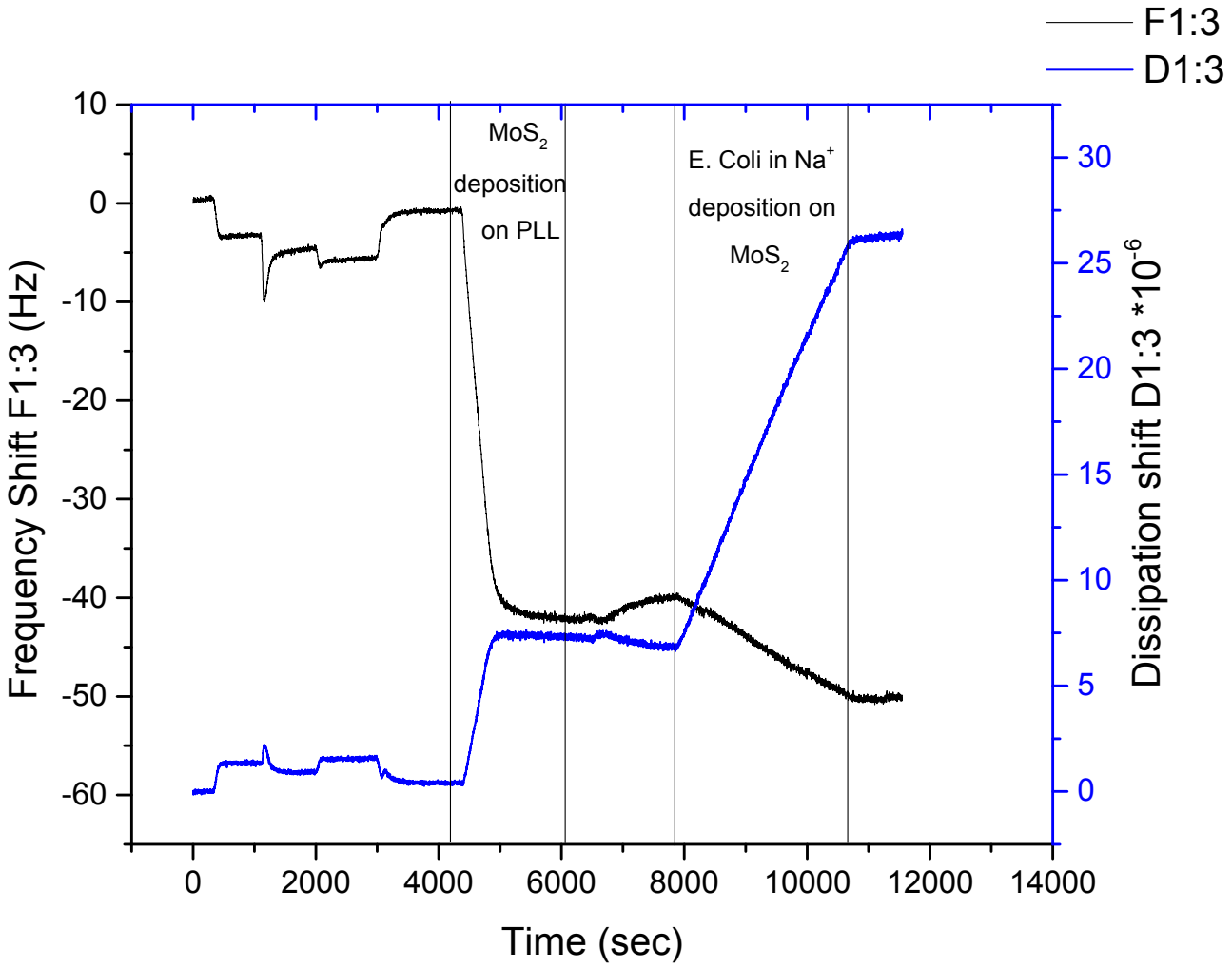

Figure S11. Real time data of the *E. coli* in NaCl deposition on a MoS_2 surface during different experiments acquired from QCM-D software tool Q-Tools. Here also, *E. coli* deposited slowly but continuously for 30 min until the *E. coli* injection was stopped and background salt solution was flowed.

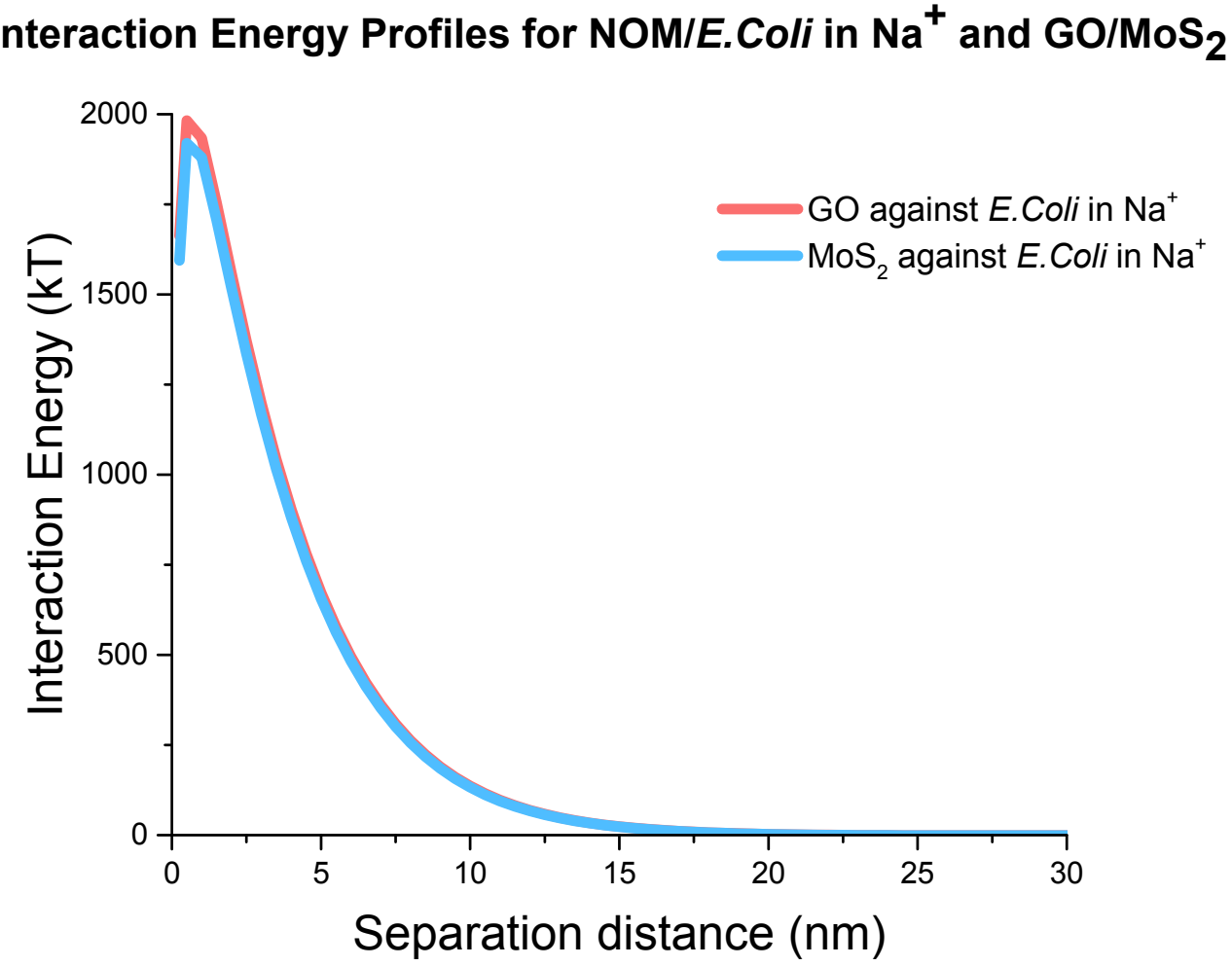

Figure S12. A high energy barrier (2000 KT) exists in the case of *E. coli* deposition in NaCl on GO and MoS_2 surfaces which supports the experimental observation of low deposition and attachment efficiency of *E. coli* to the material surfaces. This interaction energy is much higher than the average thermal energy of the particles (1.5 kT).

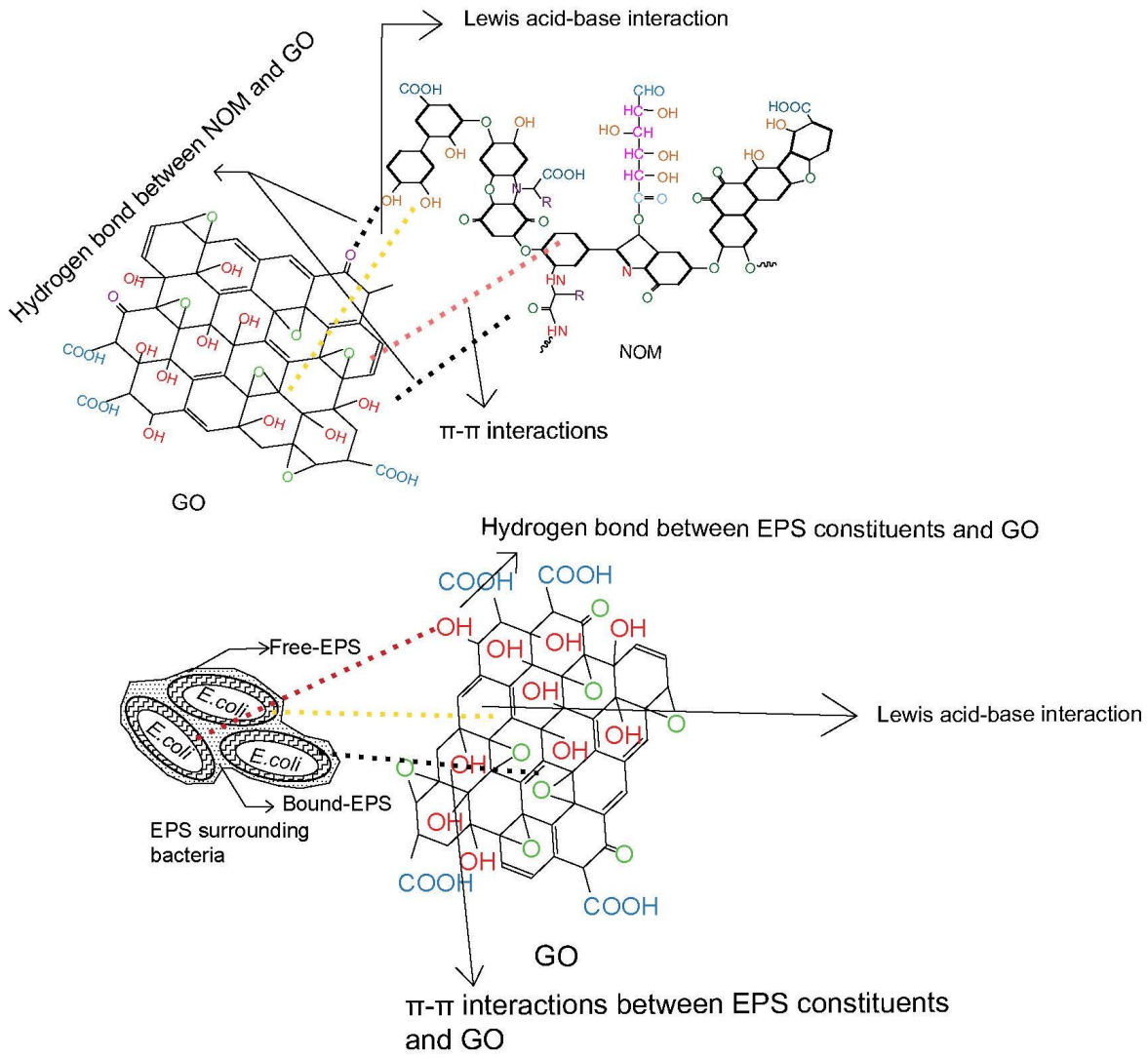

Figure S13. Mechanisms of interactions of GO with NOM and *E. coli*. Hydrogen bond between functional groups of NOM and EPS constituents, π-π interaction between aromatic rings of foulants and GO, Lewis acid-base interaction between GO center (Lewis acid) and –OH (Lewis base) functional groups of foulants etc. play significant role in foulant deposition on GO surface.

References.

1. M. C. Duch, G. R. S. Budinger, Y. T. Liang, S. Soberanes, D. Urich, S. E. Chiarella, L. A. Campochiaro, A. Gonzalez, N. S. Chandel, M. C. Hersam and G. M. Mutlu, Minimizing Oxidation and Stable Nanoscale Dispersion Improves the Biocompatibility of Graphene in the Lung, *Nano Letters*, 2011, **11**, 5201-5207.
2. I. Chowdhury, M. C. Duch, N. D. Mansukhani, M. C. Hersam and D. Bouchard, Colloidal Properties and Stability of Graphene Oxide Nanomaterials in the Aquatic Environment, *Environmental Science & Technology*, 2013, **47**, 6288-6296.
3. I. Chowdhury, M. C. Duch, N. D. Mansukhani, M. C. Hersam and D. Bouchard, Interactions of Graphene Oxide Nanomaterials with Natural Organic Matter and Metal Oxide Surfaces, *Environmental Science & Technology*, 2014, **48**, 9382-9390.
4. J. Gregory, *Particles in Water: Properties and Processes*, CRC Press, 2005.
5. R. Hogg, T. W. Healy and D. W. Fuerstenau, Mutual coagulation of colloidal dispersions, *Transactions of the Faraday Society*, 1966, **62**, 1638-1651.